Opto-Electronics Review

journal homepage: https://journals.pan.pl/opelre

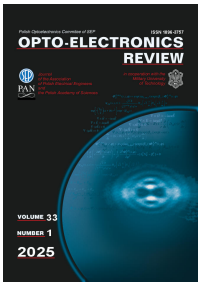

Deposition of SnO_2 as a functional layer on a porous silicon substrate for potential tandem solar cell application

Grażyna Kulesza-Matlak[1*], Marek Szindler[2], Magdalena M. Szindler[2], Anna Sypien[1], Lukasz Major[1], Kazimierz Drabczyk[1,3]

[1] Institute of Metallurgy and Materials Science, Polish Academy of Sciences, ul. Reymonta 25, 30-059 Krakow, Poland
[2] Faculty of Mechanical Engineering, Silesian University of Technology, ul. Konarskiego 18A, 44-100 Gliwice, Poland
[3] Faculty of Materials, Civil and Environmental Engineering, University of Bielsko-Biala, ul. Willowa 2, 43-309 Bielsko-Biala, Poland

Article info

Article history:
Received 23 Jul. 2024
Received in revised form 22 Oct. 2024
Accepted 11 Nov. 2024
Available on-line 23 Jan. 2024

Keywords:
tandem solar cell;
ALD;
SnO_2;
recombination layer;
silicon nanowires;
MAE etching.

Abstract

The article presents the results of a SnO_2 layer deposition, selected for its properties to function as either a recombination layer or an electron transporting material (ETM) layer in a potential silicon/perovskite tandem solar cell. The layer was deposited using an atomic layer deposition (ALD) method to ensure uniform coverage on the rough surface of etched silicon nanowires. The deposition process was monitored using test samples on glass by assessing surface roughness with an atomic force microscopy method and a total transmission through UV-VIS spectroscopy. The test layers were further characterised to estimate thickness using ellipsometry. The target layers, deposited on the porous surface of etched silicon nanowires, were examined using high-resolution scanning electron microscopy and transmission electron microscopy to evaluate the material microstructure, layer adhesion to the substrate, and the accuracy of ALD deposition on highly porous structures.

1. Introduction

The development of photovoltaic (PV) installations is continuous and undeniable. This includes ongoing technological development, cost reduction, and increased awareness of the benefits of renewable energy. It is estimated that over 90% of commercial solar cells on the market are made of silicon [1]. Crystalline silicon (c-Si) dominates due to a high efficiency of modules, a high content of silicon in the Earth's crust and a non-toxicity of its constituent elements, as well as a long-term reliability [2]. In recent years, the energy conversion efficiency in silicon solar cells has been constantly increasing thanks to the emergence of new device designs such as passivated emitter and rear cell (PERC) [3] or tunnel oxide passivated contact (TOPCon) [4]. Moreover, using interdigitated back contact (IBC) cells allows for avoiding losses resulting from surface shading [5]. However, the increase in the efficiency of a c-Si cell is limited by technological possibilities to 27% due to external recombination losses, optical losses, and the presence of resistance [6]. Moreover, Auger recombination indicates that the efficiency of a silicon PV cell is limited to a theoretical efficiency limit of 29.5 % [7].

One method of increasing the power of PV devices is to absorb solar radiation using more than one photoactive material selectively. Combining many structures that can act as a solar cell in a monolithic system leads to forming a tandem cell. In such a cell, the material with a higher band gap energy constitutes the upper tandem cell (usually in thin-film technology), and the lower cell is mostly silicon-based [8, 9]. In this way, it is possible to effectively absorb high-energy (short wavelength) photons by a high band gap cell, and the rest of the unabsorbed radiation encounters a cell with a lower band gap energy. This enables a wide solar spectrum and minimizes the thermalization process [10].

A monolithic tandem solar cell combines two sub-cells connected by an interconnecting layer (ICL) which plays a key role in charge carrier transport and recombination between sub-cells, directly influencing the device efficiency. Properly designing a functional layer is based on under-

*Corresponding author at: g.kulesza@imim.pl

https://doi.org/10.24425/opelre.2024.152685
1896-3757/ Association of Polish Electrical Engineers (SEP) and Polish Academic of Sciences (PAS). Published by PAS

standing the involved mechanisms, optoelectronic properties, and layer thickness [11–13].

The selection of an appropriate recombination layer must be dictated by the knowledge of its optical and electrical parameters. The SnO_2 layer is characterised as a well-conductive layer with a wide range of applications in tandem solar cells [14]. Mostly, the SnO_2 is used as an electron transport layer (ETL) alone [15] or doped [16]. However, scientific works are indicating that a thin SnO_2 layer deposited using an atomic layer deposition (ALD) method successfully functions as an independent recombination layer [17] is an element of a recombination bilayer [18], or serves as a buffer layer coexisting with the recombination layer [19, 20].

The presented results are fully related to the topics published in previous publications. A structure of silicon wires has been developed, which serves as a scaffold for a tandem PV structure, but initially, the wires were intended to act as a surface texture for solar cells by reducing the reflection of solar radiation from the front surface of the silicon wafer. This treatment allows for an increase in the absorption of photons necessary for the PV effect by expanding the surface and the texturization itself changes the morphology of the surface from relatively smooth to rough. The research was carried out using a metal-assisted etching method (MAE) [21]. Further on, a variant of using silicon wires as a direct scaffold for the perovskite absorber in a tandem cell was also adopted [22]. Therefore, due to the dual function of the substrate, a compromise was made between reducing solar reflection and the operational possibilities of applying subsequent layers in a tandem cell. The accepted compromise is using wires with a height in the range of 300–500 nm.

With an established methodology for fabricating a porous nanowire structure and incorporating perovskites into a tandem cell configuration, efforts were undertaken to develop a recombination layer. This layer serves as a critical interface, integrating two absorber materials into a functional tandem device. Looking at the structure of the wires, the spaces between them are narrow and long. This means that all chemical deposition methods do not work, leaving voids (air bubbles) in the structure or not allowing the same layer thickness over the entire surface to be obtained.

The attempt to obtain conductive recombination layers was performed using physical methods. For example, an indium tin oxide (ITO) layer was applied to the same wire structure using magnetron sputtering [23]. Examination of the silicon microstructure with wires and sputtered ITO layer showed that the applied layer completely covers the wires and also the spaces between the wires. Unfortunately, it forms the shape of a “match” which means that it is thicker in the upper part of the wire. This effect increases as the ITO layer thickens. Therefore, the authors attempted to obtain a layer using the ALD method on the same silicon nanowire substrate. The authors have previously employed this method with success in fabricating an anti-reflective layer [24]. Due to economic and availability reasons, the SnO_2 layer was selected.

In this study, the authors use the ALD technique to investigate the feasibility of depositing an optoelectronic layer of SnO_2 onto a silicon nanowire structure.

2. Materials

A single-crystal p-type silicon substrate was used for the work. A detailed description of silicon etching by the MAE method and the reagents used was included in previous publications on the researched topic [21]. For further work, silicon substrates of etched wires with lengths of 300–500 nm were used and obtained during etching times of 20 s.

A SnO_2 layer was deposited using the ALD method in a Picosun R-200 (Espoo, Finland) reactor. Compounds like tin chloride ($SnCl_4$) were used as a precursor. In each case, deionized water was used as a reagent. For the selected compound, the thermal ALD parameters were used with a deposition temperature of 300 °C with pulse lengths of 0.1 and 5 s, creating precursor and water, respectively. The purge step with N_2 of 5 s flowing was used between pulses to remove the remains of precursors and reaction by-products. Different sets of number of cycles of individual thin films were prepared. The number of cycles for a single SnO_2 thin film was in the range of 1000–2500 times.

3. Results

The research focuses on the possibility of depositing a functional layer in the form of SnO_2 on a porous silicon surface using the ALD method. The analysis of the deposited layers was conducted in two distinct phases. The initial phase focused on evaluating surface roughness, thickness, and optical properties of test samples deposited on microscopic glass substrates. This approach was employed to isolate and assess the intrinsic properties of the deposited layer, independent of any interactions with the underlying silicon wire structures. In the subsequent phase, a microscopic analysis was used to examine the microstructure of the layer deposited on the proposed substrate which comprised etched silicon wires.

The SnO_2 layers were examined in terms of the roughness obtained by the deposition method. For this purpose, the layers were deposited on microscope glasses, and their topography was examined using an atomic force microscopy (AFM) method. The results are presented in Fig. 1.

The surface topography of the analysed samples was evaluated using a Park System XE100 atomic force microscope (Park Systems, Suwon, South Korea) in a non-contact mode, covering areas of 2×2 μm². Both 2D images and their corresponding 3D representations were registered, alongside basic roughness parameter calculations. The cantilever vibration frequency during the test was maintained at 300 kHz. Subsequently, the acquired data was processed using the Park Systems XEI 4.3.1 program.

All test samples showed low roughness. The roughness can be higher in the initial phase of the ALD growth compared to later stages as the film thickness increases. At the beginning of the ALD process, atoms deposit onto the substrate surface, which may be uneven or contain defects, leading to increased roughness. However, these variations occur on a subatomic scale. As the process progresses, subsequent ALD cycles gradually smooth out the surface, potentially reducing roughness as the film thickness grows. This effect is particularly noticeable in materials with non-uniform early deposition stages, or the substrate has significant surface imperfections. This is consistent with the

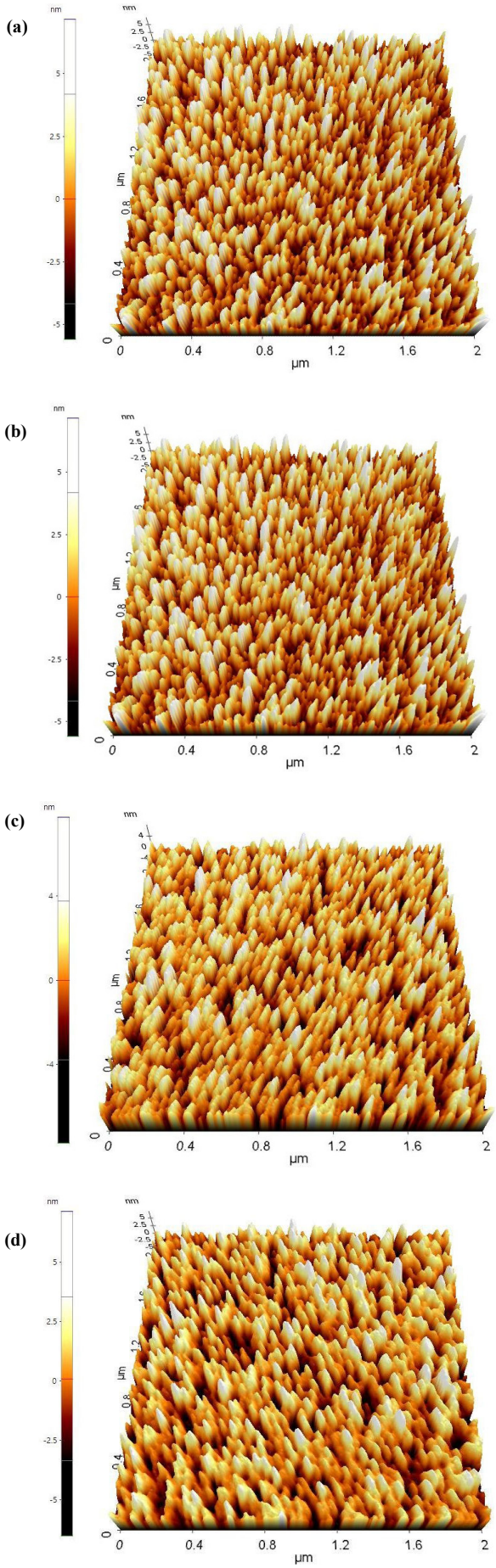

Fig. 1. AFM image of SnO_2 test layers deposited in a) 1000, b) 1500, c) 2000, d) 2500 cycles on the microscopic glass substrate.

results obtained from atomic force microscopy, as confirmed by the roughness data presented in Table 1, which shows the roughness parameters R_a and R_q as surface values from 2 µm to 2 µm.

Table 1.
SnO_2 layer roughness values estimated using the AFM method.

Roughness	1000 cycles	1500 cycles	2000 cycles	2500 cycles
R_a [nm]	1.754	1.598	1.488	1.362
R_q [nm]	2.130	1.948	1.923	1.758

The results in Table 1 confirm the low roughness of the layers deposited on the glass substrate using the ALD method. The same test layers on the same substrate were examined for their optical properties. Figure 2 shows the total transmission for SnO_2 layers depending on their thickness.

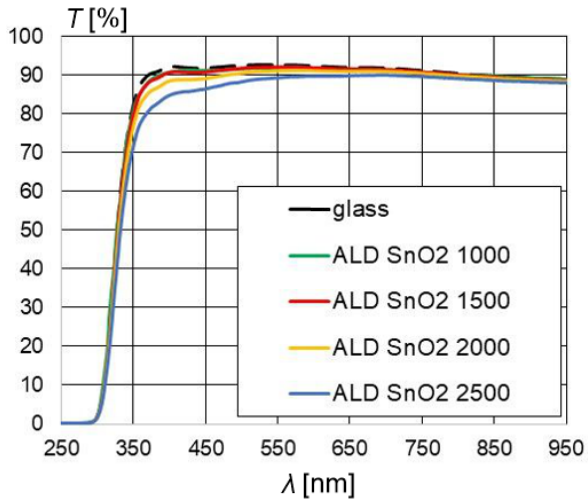

Fig. 2. Dependence of total transmission as a function of wavelength for different thicknesses of test SnO_2 layers deposited on the glass substrates.

The optical characteristics of the thin films underwent an analysis using a UV-VIS 220 Evolution spectrophotometer from Thermo Fisher Scientific (Waltham, MA, USA). Spectral measurements were conducted within the range of 250–950 nm. Transmittance was determined using an ISA-220 integrating sphere accessory.

SnO_2 layers show a very high transmission coefficient for the tested wavelength range. When comparing the total transmission values to the reference sample, i.e., microscope glass, no significant decreases in transmission are noted. A clear decrease in transmission in the wavelength range of 300–350 nm results from the lack of transmission of short-wave radiation through the glass which was the substrate. The visible absorption of the layers themselves is observed in the wavelength range of 350–550 nm where the transmission values are lower than for the reference sample and the values decrease with the layer thickness increase. Above 550 nm, the total transmission is only slightly lower than the reference sample. This means that the optical properties of the SnO_2 layer allow it to be used as an element of a tandem solar cell. The perovskite cell will first absorb the radiation falling on such a tandem. Considering

the average band gap energy values for perovskites, radiation with a shorter wavelength, up to approximately 800 nm, will be absorbed. In this situation, the long-wave radiation directed to the silicon cell cannot be lost as a result of absorption in the recombination layer (here SnO_2).

The final stage of the test samples examination was thickness modelling using the ellipsometric method. Test samples on glass substrates were measured using an SE 800 Sentech ellipsometer due to thickness examination challenges in porous samples, especially when using optical and microscopic methods. The results are presented in Table 2.

Table 2.
SnO_2 layer thickness values were estimated using the ellipsometric method.

	1000 cycles	1500 cycles	2000 cycles	2500 cycles
Thickness [nm]	4.62	8.61	12.86	18.20

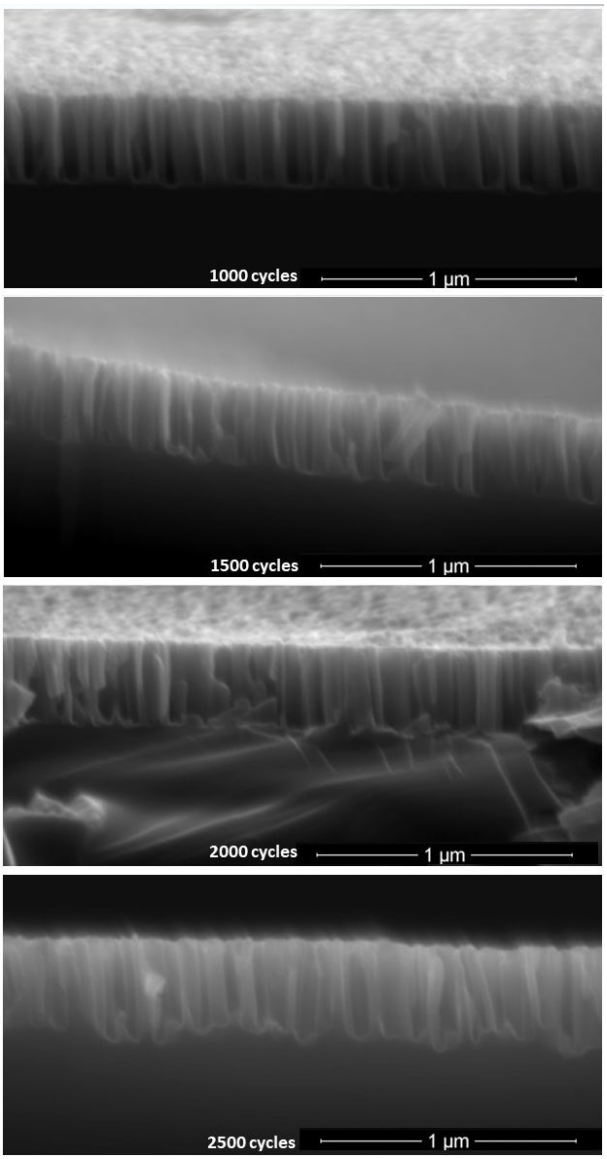

Fig. 3. SEM micrographs showing four different SnO_2 layers (with several deposition cycles equal to 1000, 1500, 2000, and 2500) deposited on a substrate consisting of wires etched in 20 s.

The next research element was to examine the SnO_2 layers deposited on the silicon nanowires substrate. The microstructure was assessed to visually check whether the applied layer is homogeneous and whether it fills the spaces between the wires. The surface morphology was examined using the scanning electron microscopy (SEM) technique using a QUANTA 200 3D Dual Beam (FEI). For a detailed study of the microstructure, a transmission electron microscopy (TEM) technique was used with Tecnai G2 F20 (200 kV) equipped with a field-emission gun (FEG) and an HAADF detector.

Firstly, SEM micrographs were taken. Figure 3 shows four types of samples differing in SnO_2 thickness. All layers were deposited on the same-prepared substrates made of silicon wires.

The deposited SnO_2 layers are homogeneous and do not tend to increase in thickness at the top of the wires. There are no visible discontinuities or voids in the applied layer. However, the SEM technique should be treated here as a general one showing that the layer is suitable for further testing with more sophisticated methods.

Therefore, the FIB technique prepared thin films, so-called lamellas for TEM observations, and TEM imaging was performed. Two samples, the thinnest (1000 cycles) and its twice equivalent (2000 cycles) layers were selected for the tests to check the presence of a layer fully covering the wires. The results are shown in Fig. 4.

TEM micrographs, performed in the bright field (BF) mode, revealed that the SnO_2 layer completely homogeneously covers the wires, and most importantly, the presence of the layer in the lower part of the wires was confirmed. The thin layer is advantageous when there are small spaces between the wires. Figure 5 compares both samples to illustrate the difference in layer thickness depending on the number of deposition cycles.

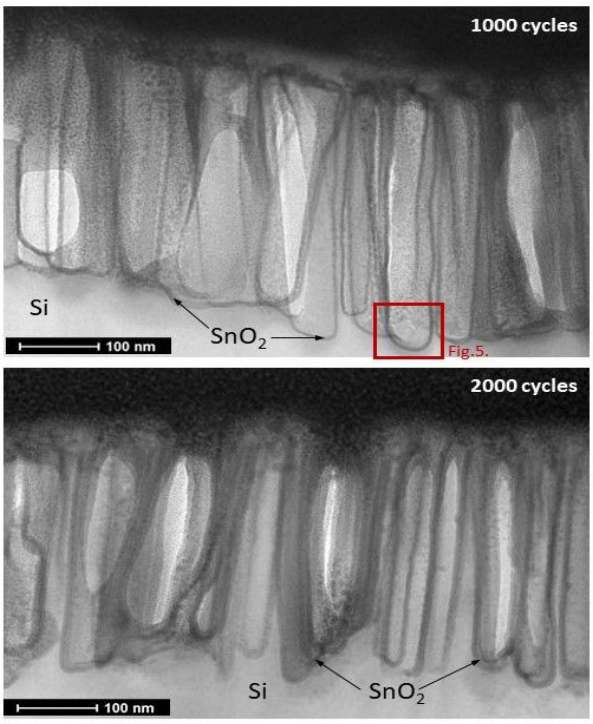

Fig. 4. BF-TEM micrograph of the SnO_2 layer deposited in 1000 and 2000 cycles placed on a substrate consisting of wires etched in 20 s.

The comparison, visible in Fig. 5, shows that the thickness of the layer deposited in the 1000 cycles mode is approximately 5 nm, while 2000 cycles of deposition allow obtaining a layer twice as thick, equal to 10 nm. The base of the wires is shown in Fig. 5 as a critical location (due to the possibility of depositing the layer at the deepest point of the rough structure), but the thickness at the top of the structure is identical.

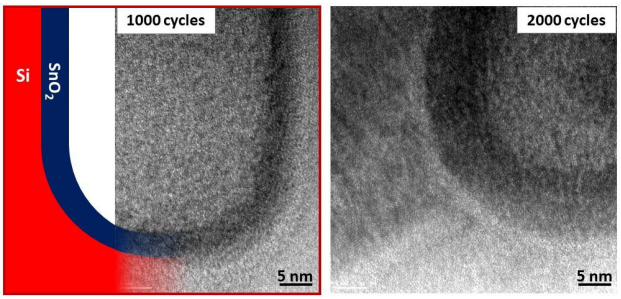

Fig. 5. HR-TEM micrograph of the SnO_2 layer deposited in 1000 and 2000 cycles placed on a substrate consisting of wires etched in 20 s.

4. Conclusions

On a substrate of silicon nanowires, chemically etched using the MAE method, a SnO_2 layer was deposited using the ALD method. The presented layer can act as a recombination or interconnecting, as well as a buffer layer in a silicon-perovskite tandem solar cell. Four layers differing in numbers of deposition cycles equal to 1000, 1500, 2000, and 2500 were tested.

The test samples were characterised by surface roughness, layer thickness, and optical properties. As a result of the AFM studies, all samples exhibited low surface roughness, decreasing with increasing layer thickness. The R_a parameter varies between 1.754 and 1.362 nm, and R_q between 2.130 and 1.758 nm. The thickness of the test films deposited on glass, estimated using the ellipsometric method, was 4.62, 8.61, 12.86, and 18.20 nm for samples deposited over 1000, 1500, 2000, and 2500 cycles, respectively. Depending on the thickness of the SnO_2 layer, its optical properties were examined, which are characterized by high transmission in the wavelength range above 550 nm, i.e., for radiation that should be effectively transmitted to the lower cell, in this case, silicon. The total transmission in this range is approximately 90%.

Studies of the microstructure of silicon with wires and a deposited SnO_2 layer showed that the layer completely covers the wires in the spaces between the wires uniformly without changes in thickness in the upper or lower part of the wire. The thickness of the thinnest SnO_2 layer (1000 cycles) is estimated at approx. 5 nm, while the layer applied in twice the number of cycles is twice as thick, equal to 10 nm.

The presented research should be treated as an optimistic introduction to further tests of the layers themselves from an electrical perspective, as well as the fulfilment of the functionality assigned to them in the entire tandem structure.

Acknowledgements

This research was funded by IMMS PAS as a statutory work. The SEM and TEM examinations were performed in the Accredited Testing Laboratories at the IMMS PAS (ILAC-MRA).

References

[1] Di Sabatino, M., Hendawi, R. T. A. & Garcia, A. S. Silicon solar cells: Trends, manufacturing challenges, and AI perspectives. *Crystals* **14**, 167 (2024). https://hdl.handle.net/11250/3153161

[2] Fu, F. *et al*. Monolithic perovskite-silicon tandem solar cells: from the lab to fab? *Adv. Mater*. **34**, 2106540 (2022). https://doi.org/10.1002/adma.202106540

[3] Blakers, A. Development of the PERC solar cell. *IEEE J. Photovolt.* **9**, 629–635 (2019). https://doi.org/10.1109/JPHOTOV.2019.2899460

[4] Kafle, B. *et al*. TOPCon – Technology options for cost efficient industrial manufacturing. *Sol. Energy Mater. Sol. Cells* **227**, 111100 (2021). https://doi.org/10.1016/j.solmat.2021.111100

[5] Smith, D. D. *et al*. Toward the practical limits of silicon solar cells. *IEEE J. Photovolt.* **4**, 1465–1469 (2014). https://doi.org/10.1109/JPHOTOV.2014.2350695

[6] Yoshikawa, K. *et al*. Silicon heterojunction solar cell with interdigitated back contacts for a photoconversion efficiency over 26%. *Nat. Energy* **2**, 17032 (2017). https://doi.org/10.1038/nenergy.2017.32

[7] Schäfer, S. & Brendel, R. Accurate calculation of the absorptance enhances efficiency limit of crystalline silicon solar cells with Lambertian light trapping. *IEEE J. Photovolt.* **8**, 1156 (2018). https://doi.org/10.1109/JPHOTOV.2018.2824024

[8] Xu, Q. J. Zhao, Y. & Zhang, X. Light management in monolithic perovskite/silicon tandem solar cells. *Sol. RRL* **4**, 1900206 (2020). https://doi.org/10.1002/solr.201900206

[9] Hu, Y., Chen, Y. & Huang, W. Two-terminal perovskites tandem solar cells: Recent advances and perspectives. *Sol. RRL* **3**, 1900080 (2019). https://doi.org/10.1002/solr.201900080

[10] Jošt, M, Kegelmann, L. & Albrecht, S. Monolithic perovskite tandem solar cells: a review of the present status and advanced characterization methods toward 30% efficiency. *Adv. Energy Mater*. **10**, 1904102 (2020). https://doi.org/10.1002/aenm.201904102

[11] Xie, Y.-M. *et al*. Understanding the role of interconnecting layer on determining monolithic perovskite/organic tandem device carrier recombination properties. *J. Energy Chem*. **71**, 12–19 (2022). https://doi.org/10.1016/j.jechem.2022.03.019

[12] Zang, Y. *et al*. Optical design of monolithic two-terminal perovskite/Si tandem solar cells for efficient photon management. *Mater. Today Commun*. **38**, 108199 (2024). https://doi.org/10.1016/j.mtcomm.2024.108199

[13] Zheng, J. *et al*. Balancing charge-carrier transport and recombination for perovskite/TOPCon tandem solar cells with double-textured structures. *Adv. Energy Mater*. **13**, 2203006 (2023). https://doi.org/10.1002/aenm.202203006

[14] Mazumdar, S., Zhao, Y. & Zhang, X. Comparative architecture in monolithic perovskite/silicon tandem solar cells. *Sci. China: Phys. Mech. Astron*. **66**, 217304 (2023). https://doi.org/10.1007/s11433-022-1928-8

[15] Howlader, A. H. *et al*. Self-formation of $SnCl_2$ passivation layer on SnO_2 electron-transport layer in chloride-iodide-based perovskite solar cell. *Adv. Energy Sustain. Res*. **5**, 2400030 (2024). https://doi.org/10.1002/aesr.202400030

[16] Zeng, Q. *et al*. Hysteresis-free perovskite solar cells with over 24% efficiency enabled by $ZnCl_2$ doped SnO_2 electron transfer layer. *Appl. Phys. Lett*. **124**, 033901 (2024). https://doi.org/10.1063/5.0186904

[17] McDonald, C. *et al*. *In situ* grown nanocrystalline Si recombination junction layers for efficient perovskite–Si monolithic tandem solar cells: Toward a simpler multijunction architecture. *ACS Appl. Mater. Interfaces* **14**, 33505–33514 (2022). https://doi.org/10.1021/acsami.2c05662

[18] Bush, K. A. *et al*. 23.6%-efficient monolithic perovskite/silicon tandem solar cells with improved stability. *Nat. Energy* **2**, 17009 (2017). https://doi.org/10.1038/nenergy.2017.9

[19] Li, C., Wang, Y. & Choy, C. H. Efficient interconnection in perovskite tandem solar cells. *Small Methods* **4**, 2000093 (2020). https://doi.org/10.1002/smtd.202000093

[20] Mariotti, S. *et al*. Monolithic perovskite/silicon tandem solar cells fabricated using industrial p-type polycrystalline silicon on oxide/passivated emitter and rear cell silicon bottom cell technology. *Sol. RRL* **6**, 2101066 (2022). https://doi.org/10.1002/solr.202101066

[21] Kulesza-Matlak, G. *et al*. Black silicon obtained in two-step short wet etching as a texture for silicon solar cells-surface microstructure and optical properties studies. *Arch. Metall. Mater*. **63**, 1009–1017 (2018). https://doi.org/10.24425/122436

[22] Kulesza-Matlak, G. *et al*. Interlayer microstructure analysis of the transition zone in the silicon/perovskite tandem solar cell. *Energies* **14**, 6819 (2021). https://doi.org/10.3390/en14206819

[23] Kulesza-Matlak, G. *et al*. Morphology of an ITO recombination layer deposited on a silicon wire texture for potential silicon/perovskite tandem solar cell applications. *Opto-Electron. Rev.* **31**, e148222 (2023). https://doi.org/10.24425/opelre.2023.148222

[24] Szindler, M. *et al*. The Al2O3/TiO2 double antireflection coating deposited by ALD method. *Opto-Electron. Rev.* **30**, e141952 (2022). https://doi.org/10.24425/opelre.2022.141952